Paleoceanography and Paleoclimatology

Supporting Information for

Persistent link between Caribbean precipitation and Atlantic Ocean circulation during the Last Glacial revealed by a speleothem record from Puerto Rico

Sophie F. Warken[1,2,3*], Rolf Vieten[4], Amos Winter[4,5], Christoph Spötl[6], Thomas E. Miller[7], Klaus P. Jochum[8], Andrea Schröder-Ritzrau[2], Augusto Mangini[2], and Denis Scholz[1]

[1] Institute for Geosciences, University of Mainz, Germany; [2] Institute of Environmental Physics, University of Heidelberg, Germany; [3] Institute of Earth Sciences, Heidelberg University, Germany; [4] Department of Marine Sciences, University of Puerto Rico, Mayagüez, Puerto Rico [5] Earth and Environmental Systems Department, Indiana State University, Terre Haute, Indiana, USA [6] Institute of Geology, University of Innsbruck, Austria; [7] Department of Geology, University of Puerto Rico, Mayagüez, Puerto Rico; [8] Max Planck Institute for Chemistry, Climate Geochemistry Department, Mainz, Germany

Contents of this file

Additional Supporting Information (Files uploaded separately)

Introduction

This supporting material contains several parts. Figure S 1 is a map of Larga Cave and indicates the location of stalagmite PR-LA-1. We also present additional information on the chronology of speleothem PR-LA-1, i.e., the results of the linear fits for each Osmond isochron (Table S 1 and Figure S 2) as well as the activity ratios and calculated ages of stalagmite PR-LA-1 (Table S 2, uploaded as separate file). In addition, results and discussion of the numerical simulations of the observed proxy variability using I-STAL (Stoll et al., 2012), ISOLUTION 1.0 (Deininger & Scholz, 2019) and REDFIT (Schulz & Mudelsee, 2002) are included. The supporting text S1 as well as Figures S3 and S4 show the results of the proxy process simulations. Figures S5 and S6 indicate the spectral power distributions for different intervals of the PR-LA-1 $\delta^{13}C$ and Mg/Ca records.

Figure S1. Map of Larga cave and location of stalagmite PR-LA-1, Puerto Rico (red symbol). The sample was collected from the main passage. After Miller (2010).

35

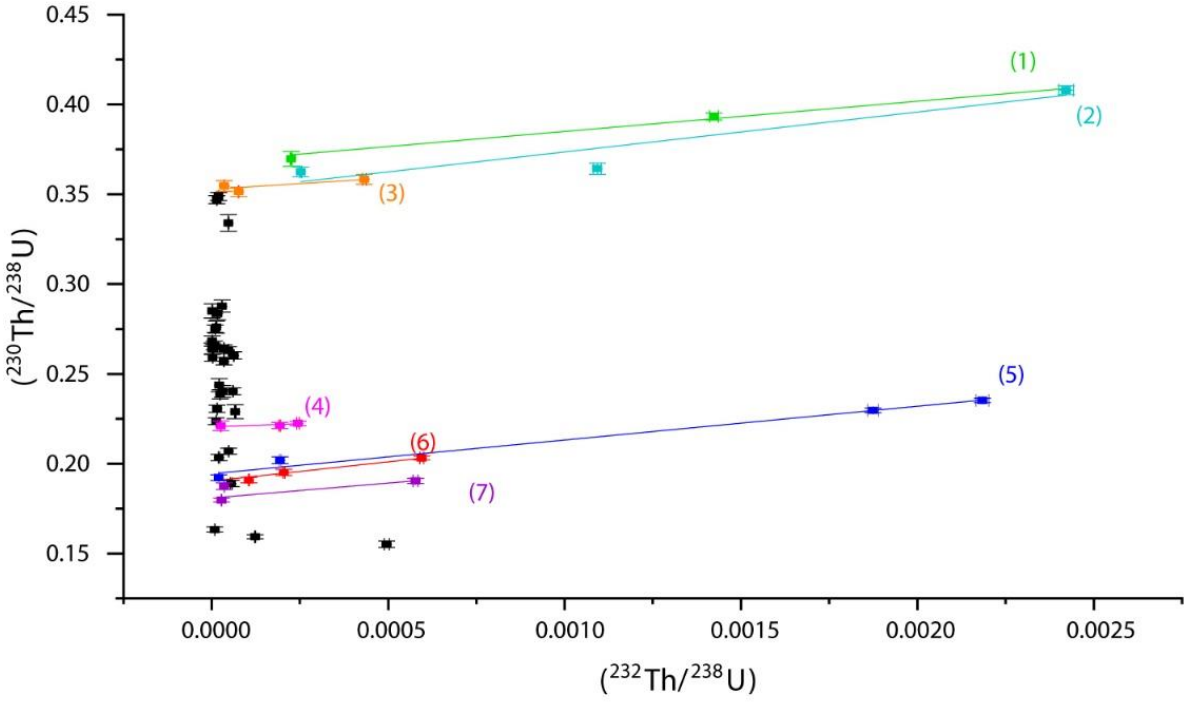

40 **Figure S2. Measured ($^{230}Th/^{238}U$) vs. ($^{232}Th/^{238}U$) activity ratios in stalagmite PR-LA-1. Different colours correspond to the individual Osmond type I isochrons and data points (Table S1).**

Table S1. Results of the linear fits for each Osmond isochron shown in Figure S 2.

# Isochron	Slope	Error	Pearson's r	N
1	16.81	± 2.08	0.99	3
2	22.22	± 7.23	0.93	3
3	12.38	± 6.70	0.85	5
4	7.04	± 14.02	0.72	3
5	18.78	± 1.42	0.99	4
6	21.35	± 2.90	0.97	4
7	16.67	± 10.64	0.72	3
Overall mean:	**16.46**	**10.58**		
For r > 0.9	**19.79**	**4.93**		

Table S2 (uploaded separately). Activity ratios and calculated ages of stalagmite PR-LA-1. Activity ratios corrected for initial Th assuming an detrital weight ratio $^{232}Th/^{238}U$ = 0.154 ± 0.038 (corresponding to an activity ratio of the detritus in secular equilibrium of $(^{230}Th/^{232}Th)_{detr}$ = 19.79 ± 4.93). Ages are calculated using the decay constants of Cheng et al. (2000). Uncertainties are given at the 2σ-level, and do not include half-life uncertainties.

Text S1. Simulation of the observed proxy variability

Inverse modelling of elemental variations using I-STAL

In order to explore drivers of trace element variability in PR-LA-1, the inverse model I-STAL was applied, similarly as described in Stoll et al. (2012). To evaluate changes on centennial to millennial timescales, the records of Mg/Ca, Sr/Ca and Ba/Ca were reduced to 100-year average values. The choice of model input parameters is closely oriented on observed variations during the cave monitoring and in the speleothem. The recorded increase of element to calcium ratios towards 15.4 ka gives the order of magnitude of the degree of enrichment by PCP of Mg, Sr and Ba, which is set to a factor of 5 (Mg), 2 (Sr) and 3 (Ba), respectively. Ca concentrations at drip sites in Larga Cave today are between 50 to 75 ppm. The range for drip intervals was set to 1 to 5000 s. We suggest that the strongest enrichment due to PCP occurs for extremely low flow, so the drip interval of maximum water-rock exchange is set to 5000 s. Cave temperature was set to 20°C, accounting for the observed mean temperature difference between the Holocene and the LGM in the region (e.g., Arienzo et al. (2015); Lea et al. (2003)).

In a first simulation, initial Ca was set to 50 ppm, and the model was run to optimize for drip interval and pCO_2. In the next step, unphysically low cave air pCO_2 values of less than atmospheric pCO_2 during the Last Glacial were set to this lower limit of 180 ppm, and the model was run to optimize for drip interval and initial Ca. This simulation was repeated for different parametrizations of e.g., baseline of initial Ca, maximum drip interval or the degree of enrichment by PCP. However, despite small absolute shifts in the mean values, the temporal variability of the modelled drip intervals and the degree of supersaturation remained relatively unaffected by the choice of variables and is therefore here only displayed for an example set of input parameters (Figure S 4). A second run first optimizing drip interval and initial Ca, and in a second step pCO_2 led to similar results. The modelled drip intervals vary over 5 orders of magnitude between 1 and 10000 s, whereas highest drip intervals were reached in the last phase of the record after 17.5 ka. In the same period, calcite supersaturation is at its lowest values.

All simulations modelled stalagmite Sr/Ca and Mg/Ca ratios well, while Ba/Ca variations are poorly reproduced. Average simulated growth rates are in the range of values as suggested by the age model (10 to 1000 µm/a).

Sensitivity simulation of processes influencing speleothem stable isotope composition

The range of the main parameters simulated by I-STAL was selected to evaluate the influence of temperature, drip interval and state of supersaturation on the speleothem $\delta^{18}O$ and $\delta^{13}C$ values using ISOLUTION 1.0 (Deininger & Scholz, 2019) and the isotopic fractionation factor of Tremaine et al. (2011). Unless stated otherwise, cave temperature was set to 20°C, drip water pCO_2 to 5000 ppm, cave air pCO_2 to 300ppmv, relative humidity (rH) to 99%, wind speed to 0 m/s and the mixing parameter Φ to 1. In agreement with the monitoring results, drip water $\delta^{18}O$ and $\delta^{13}C$ values were set to -2.6 and -13‰, respectively. Figure A2 shows that, keeping all other parameters constant, speleothem $\delta^{18}O$ and $\delta^{13}C$ values increase with the drip interval and the degree of supersaturation of the drip water, reaching a maximum isotope fractionation of the calcite up to +1.5‰ ($\delta^{18}O$) and 1.2‰ ($\delta^{13}C$) compared to equilibrium conditions.

While temperature has only a small impact on carbon isotope fractionation, a decrease in cave air temperature by 5°C may account for a +1‰ increase in $\delta^{18}O$ values. Evaporation effects can strongly influence the isotopic composition of the calcite. However, at high drip rates, already a moderate reduction of rH by 5% would lead to an increase of more than +1‰ in $\delta^{18}O$ and +2‰ in $\delta^{13}C$.

Combining all these effects, leads to $\delta^{18}O$ values of the calcite between -1.6 and -1.1‰ for a drip interval of 10,000s, T = 17.5°C, rH = 90% and drip water pCO_2 values of 975 and 3000ppmv, corresponding to initial Ca concentrations of 30 and 50 ppm, respectively. A temperature decrease of 15°C would further increase this value to -0.7‰. $\delta^{13}C$ values increase to a maximum of -11‰ in these

scenarios. Under these extreme conditions, the highest measured values in the speleothem of +2‰ ($\delta^{18}O$) and -4‰ ($\delta^{13}C$) can only be reproduced with drip water values of about 0‰ for $\delta^{18}O$ and -6‰ for $\delta^{13}C$, respectively.

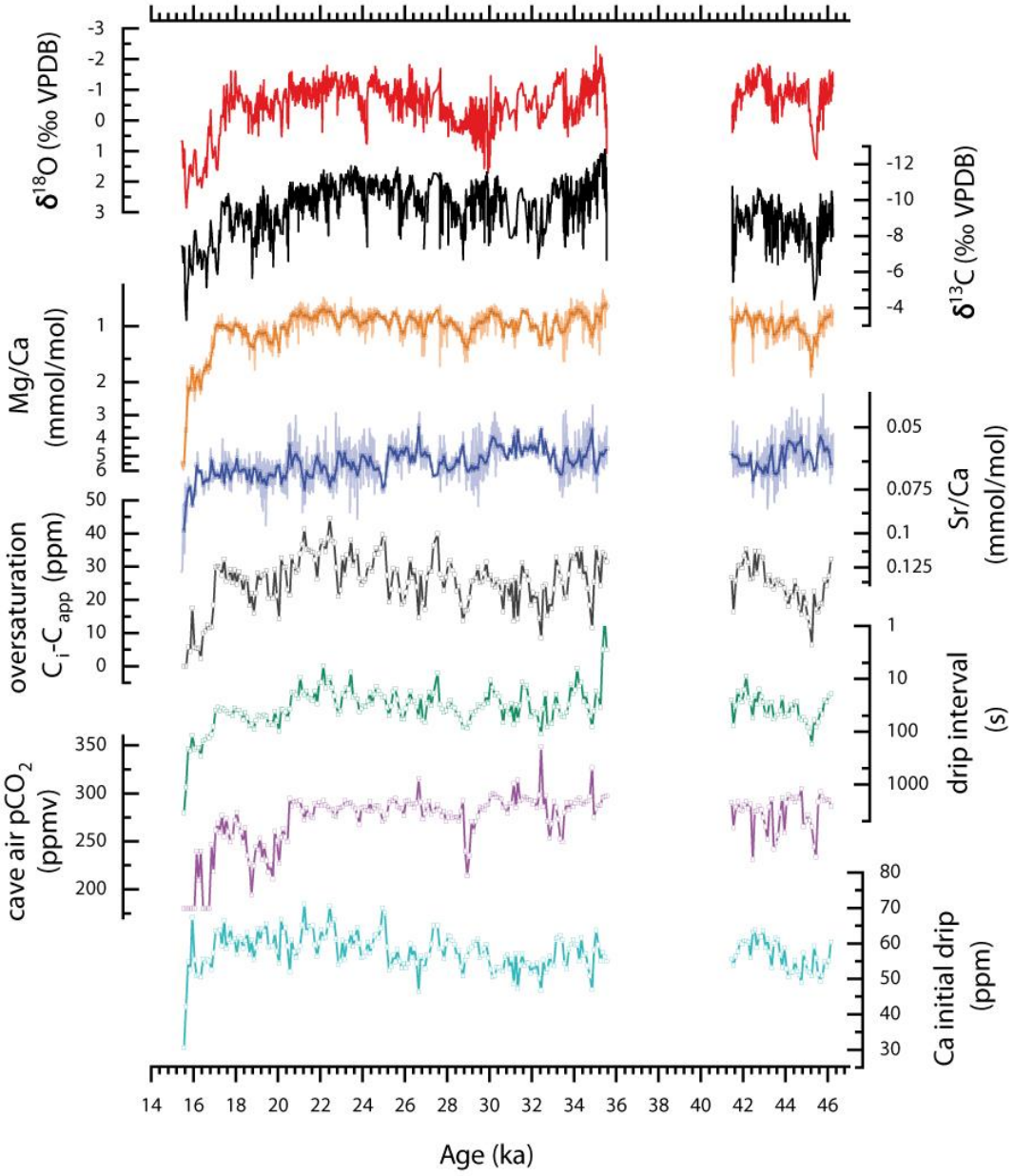

Figure S3. Results of I-STAL simulations for speleothem PR-LA-1 compared to speleothem proxies. Top panels: stable isotopes of oxygen ($\delta^{18}O$ in ‰ (red) and carbon ($\delta^{13}C$ in ‰, black), molar trace element to calcium ratios: Mg/Ca (orange), Sr/Ca (blue). Light coloured lines are the raw speleothem data, dark coloured lines interpolated to 100 y average values. Open symbols indicate modelled Mg/Ca and Sr/Ca ratios. Bottom panels: calculated oversaturation of the drip (grey), drip interval (green), cave air pCO_2 (purple) and initial Ca concentration of the drip water (turquoise).

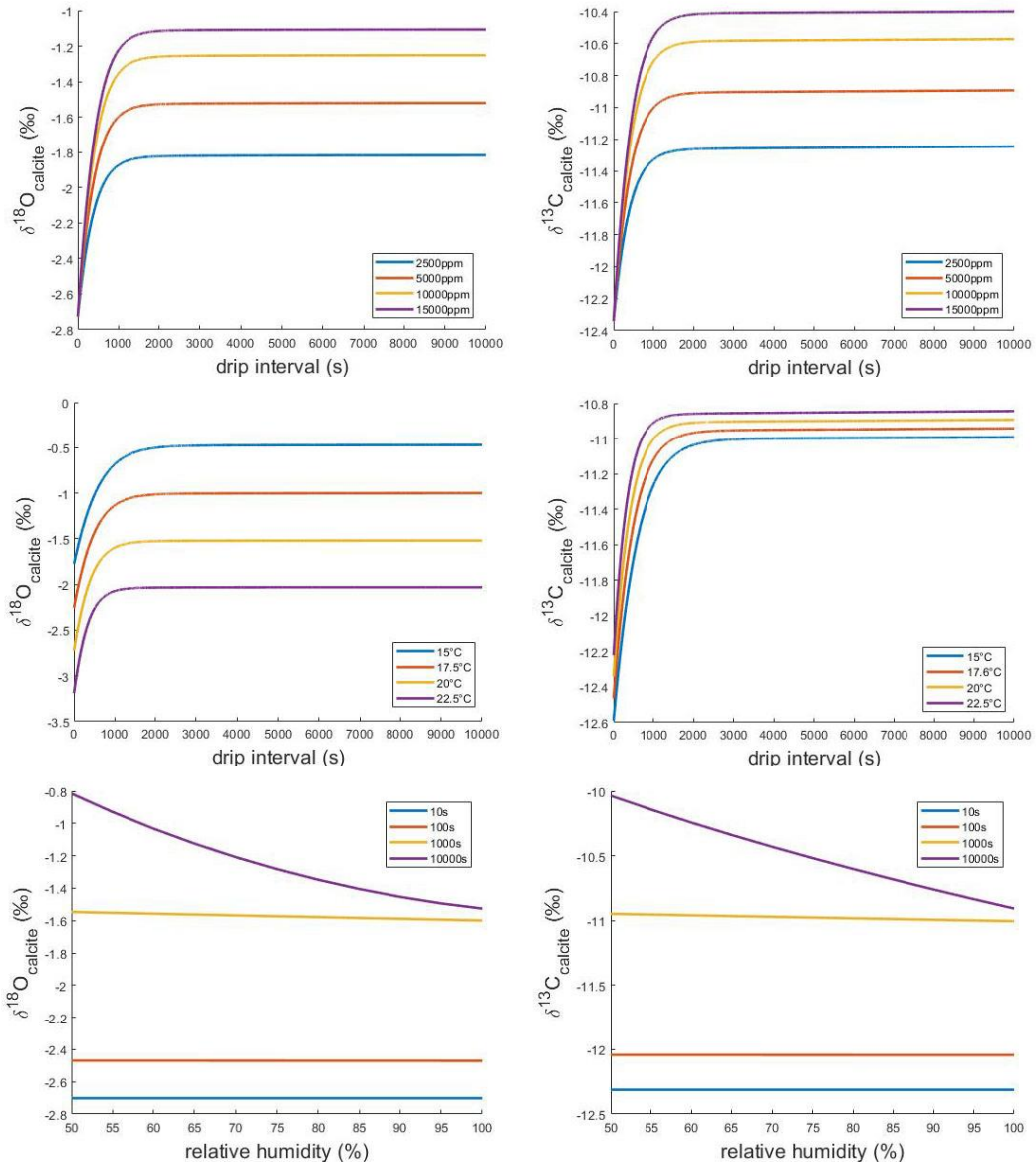

Figure S4. Simulations of the stable isotopic composition of calcite assuming initial drip water values of $\delta^{18}O$ of -2.6‰ (VSMOW) and $\delta^{13}C$ of -13 ‰. Unless stated otherwise in the individual plots, cave temperature was set to 20°C, drip water pCO_2 to 5000ppm, cave air pCO_2 to 300ppmv, relative humidity to 99%, wind speed to 0 m/s and the mixing parameter Φ to 1. All simulations calculated with ISOLUTION 1.0 (Deininger & Scholz, 2019), assuming a temperature-dependent isotope fractionation after Tremaine et al. (2011).

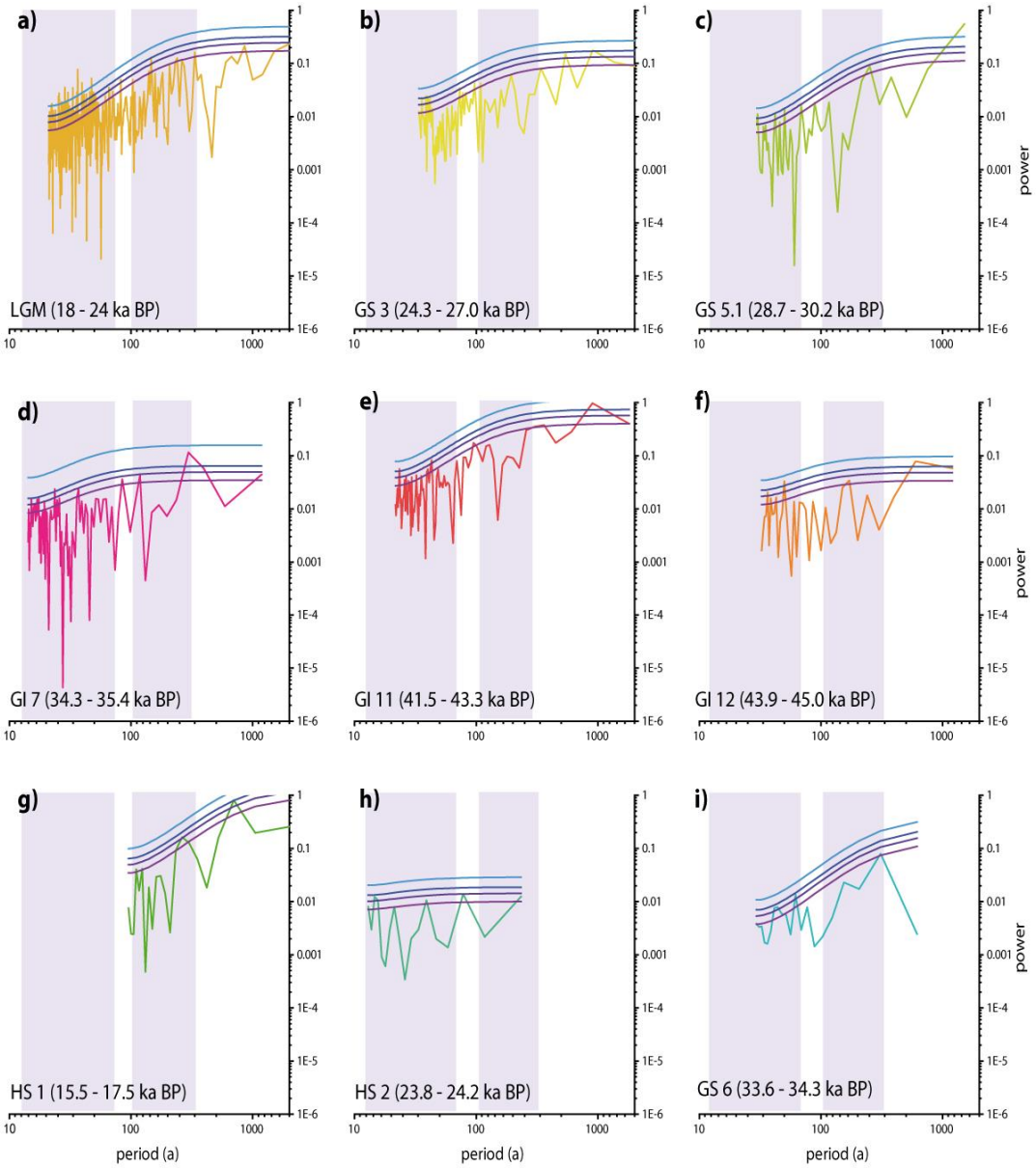

120 **Figure S5. Spectral power for different intervals of the PR-LA-1 $\delta^{13}C$ record calculated with REDFIT (Schulz & Mudelsee, 2002). Coloured lines indicate the calculated AR(1) false-alarm levels of 80% (purple), 90% (violet), 95% (dark blue) and 99% (light blue). Purple rectangles indicate the multi-decadal and centennial period bands. For all shown spectra, the AR(1) passed the REDFIT runs test which checks the equality of theoretical AR(1) and data spectrum.**

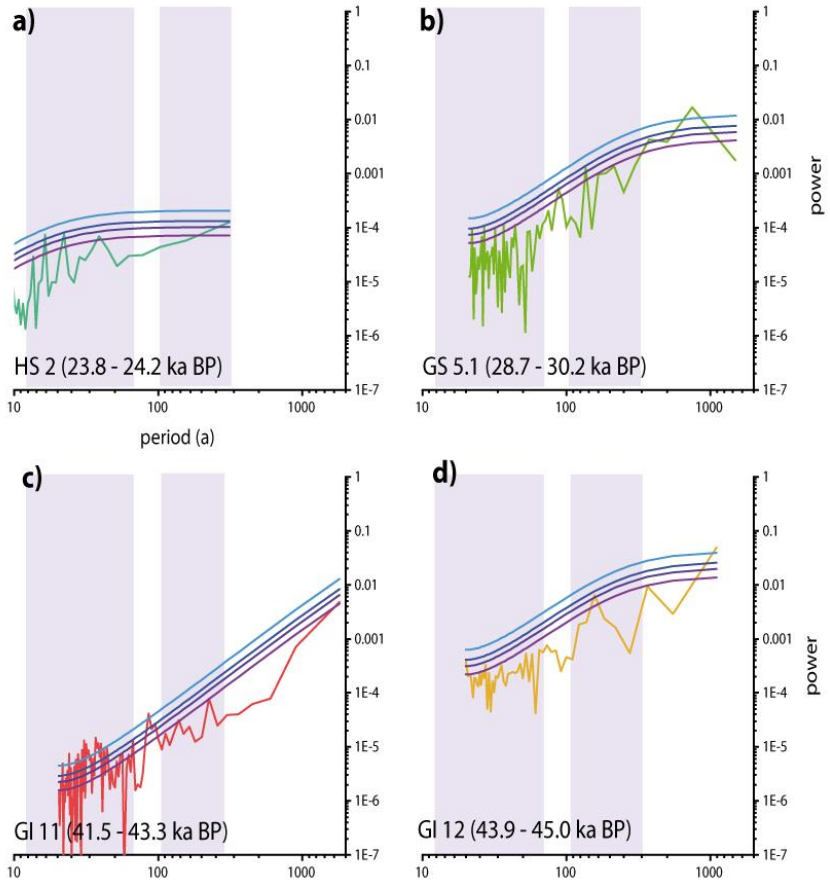

Figure S6. Spectral power for different intervals of the PR-LA-1 Mg/Ca record calculated with REDFIT (Schulz & Mudelsee, 2002). Coloured lines indicate the calculated AR(1) false-alarm levels of 80% (purple), 90% (violet), 95% (dark blue) and 99% (light blue). Purple rectangles indicate the multi-decadal and centennial period bands. For all shown spectra, the AR(1) passed the REDFIT runs test which checks the equality of theoretical AR(1) and data spectrum. For Mg/Ca, an appropriate AR(1) model could be only fitted for HS2, GS5.1 and GI 11 and 12.

References

Arienzo, M. M., Swart, P. K., Pourmand, A., Broad, K., Clement, A. C., Murphy, L. N., et al. (2015). Bahamian speleothem reveals temperature decrease associated with Heinrich stadials. *Earth and Planetary Science Letters, 430*, 377-386. doi:10.1016/j.epsl.2015.08.035

Cheng, H., Edwards, R. L., Hoff, J., Gallup, C. D., Richards, D. A., & Asmerom, Y. (2000). The half-lives of uranium-234 and thorium-230. *Chemical Geology, 169*(1-2), 17-33. doi:10.1016/s0009-2541(99)00157-6

Deininger, M., & Scholz, D. (2019). ISOLUTION 1.0: an ISOtope evoLUTION model describing the stable oxygen (δ 18 O) and carbon (δ 13 C) isotope values of speleothems. *International Journal of Speleology, 48*(1), 3.

Lea, D. W., Pak, D. K., Peterson, L. C., & Hughen, K. A. (2003). Synchroneity of tropical and high-latitude Atlantic temperatures over the last glacial termination. *Science, 301*(5638), 1361-1364. doi:10.1126/science.1088470

Miller, T. E. (2010). Stream Pirates of the Caribbean: Tanamá and Camuy Rivers in the Northern Karst of Puerto Rico. *Espeleorevista Puerto Rico, 2*, 8-13.

Schulz, M., & Mudelsee, M. (2002). REDFIT: estimating red-noise spectra directly from unevenly spaced paleoclimatic time series. *Computers & Geosciences, 28*(3), 421-426.

Stoll, H. M., Müller, W., & Prieto, M. (2012). I-STAL, a model for interpretation of Mg/Ca, Sr/Ca and Ba/Ca variations in speleothems and its forward and inverse application on seasonal to millennial scales. *Geochemistry, Geophysics, Geosystems, 13*(9). doi:10.1029/2012gc004183

Tremaine, D. M., Froelich, P. N., & Wang, Y. (2011). Speleothem calcite farmed in situ: modern calibration of δ18O and δ13C paleoclimate proxies in a continuously-monitored natural cave system. *Geochimica et Cosmochimica Acta, 75*(17), 4929-4950.